SCIENTIFIC REPORTS

OPEN

CONFERENCE PROCEEDINGS

APEnergy2014

SUBJECT AREAS:
BATTERIES
ELECTRONIC DEVICES

Received
27 February 2014

Accepted
15 July 2014

Published
29 August 2014

Correspondence and requests for materials should be addressed to J.W. (jiazhao@uow.edu.au)

Novel Germanium/Polypyrrole Composite for High Power Lithium-ion Batteries

Xuanwen Gao[1], Wenbin Luo[1], Chao Zhong[1], David Wexler[2], Shu-Lei Chou[1], Hua-Kun Liu[1], Zhicong Shi[3], Guohua Chen[3,4], Kiyoshi Ozawa[5] & Jia-Zhao Wang[1]

[1]Institute for Superconducting and Electronic Materials, University of Wollongong, Wollongong, NSW 2522, Australia, [2]School of Mechanical, Materials and Mechatronic Engineering, University of Wollongong, Wollongong, NSW 2522, Australia, [3]Centre for Green Products and Processing Technologies, Guangzhou HKUST Fok Ying Tung Research Institute, Guangzhou, China, [4]Department of Chemical and Biomolecular Engineering, The Hong Kong University of Science and Technology, Clear Water Bay, Kowloon, Hong Kong, China, [5]National Institute for Materials Science, 1-2-1 Sengen, Tsukuba-city Ibaraki 305-0047, Japan.

Nano-Germanium/polypyrrole composite has been synthesized by chemical reduction method in aqueous solution. The Ge nanoparticles were directly coated on the surface of the polypyrrole. The morphology and structural properties of samples were determined by X-ray diffraction, scanning electron microscopy and transmission electron microscopy. Thermogravimetric analysis was carried out to determine the polypyrrole content. The electrochemical properties of the samples have been investigated and their suitability as anode materials for the lithium-ion battery was examined. The discharge capacity of the Ge nanoparticles calculated in the Ge-polypyrrole composite is 1014 mAh g^{-1} after 50 cycles at 0.2 C rate, which is much higher than that of pristine germanium (439 mAh g^{-1}). The composite also demonstrates high specific discharge capacities at different current rates (1318, 1032, 661, and 460 mAh g^{-1} at 0.5, 1.0, 2.0, and 4.0 C, respectively). The superior electrochemical performance of Ge-polypyrrole composite could be attributed to the polypyrrole core, which provides an efficient transport pathway for electrons. SEM images of the electrodes have demonstrated that polypyrrole can also act as a conductive binder and alleviate the pulverization of electrode caused by the huge volume changes of the nanosized germanium particles during Li^+ intercalation/de-intercalation.

Rechargeable lithium-ion batteries are currently leading candidates for powering electric vehicles and portable electronic devices. Although such batteries have gained commercial success, their capacity is still limited by the amount of lithium that can be stored in the anode (graphite) and cathode ($LiCoO_2$) electrodes, which have theoretical lithium-ion storage capacities of 372 mAh/g and 137 mAh/g, respectively[1,2]. Therefore, intensive research efforts are continuing in the search for battery electrode materials with higher energy densities, long cycle life, and high reversible capacity[3]. Recently, as an alternative to the traditional graphitic anode materials, the Group IV metals (Sn, Ge, Si) have been considered as ideal candidate anode materials for reversible lithium energy storage due to their significantly higher lithium-ion storage capacities[4–6]. In 2005, Sony released a new lithium-ion battery system, which used Sn-Co-C composite as its anode material. This further accelerated the interest in anode electrodes made from metal or alloy.

Among these Group IV metals, germanium, with high theoretical capacity (1600 mAh g^{-1} compared with 372 mAh g^{-1} for graphite), good lithium diffusivity (400 times faster than in silicon), and high electrical conductivity (104 times higher than silicon), has been proved to be one of the most attractive potential anode materials for lithium-ion batteries. Consequently, many researchers have tried to fabricate Ge nanoparticles for battery application[7,8]. It has been widely recognized that reduction of the Ge particle size could enhance the electrochemical activity of Ge due to its shorter electron paths and larger reaction surface. Unfortunately, similarly to silicon[4] and tin[9], nanosized Ge particles always aggregate severely and merge into micron-sized particles during Li-ion insertion/extraction processes. This aggregation will lead to severe pulverization and delamination on the surface of the electrode, and a rapid decline in the electrochemical capacity[10,11]. Up to now, various strategies have been devised in attempts to overcome this issue. In general, this aggregation can be partially hindered by mixing the Ge with a large amount of carbon-based materials, such as carbon black[5,12], carbon nanotubes[13,14], and graphene[15,16].

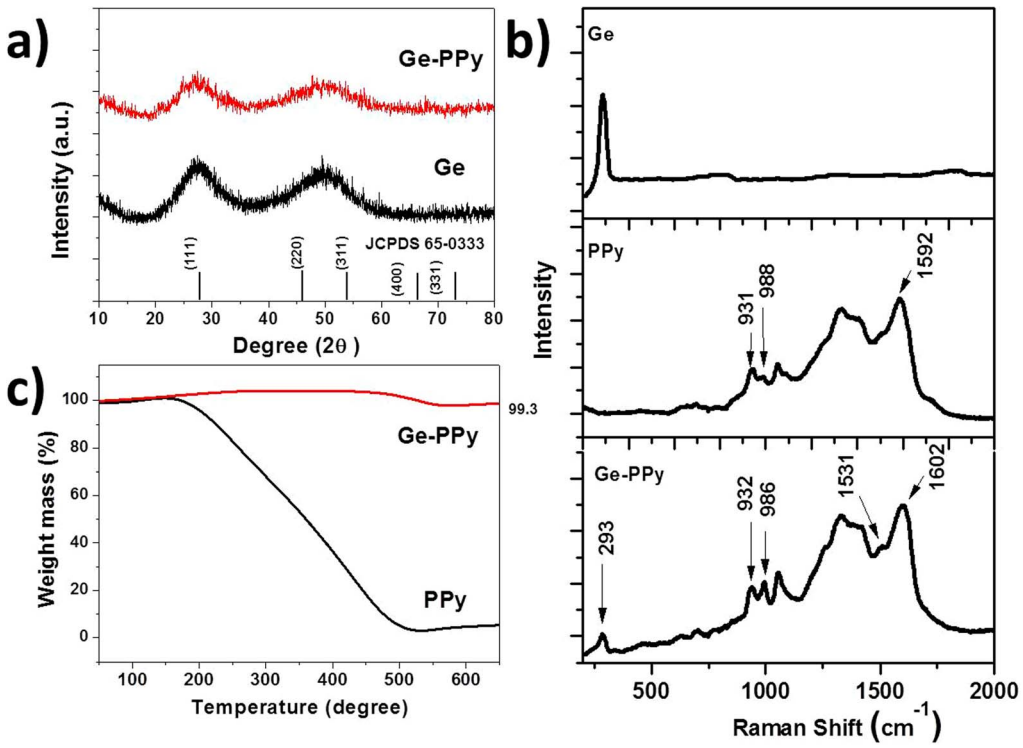

Figure 1 | (a) XRD patterns obtained from the as-prepared Ge particles and Ge-PPy composite. (b) Raman spectra of PPy, Ge and Ge-PPy composite. (c) TGA curves of PPy and Ge-PPy.

Recently, conductive polypyrrole (PPy) has attracted much attention as another effective additive material to improve the performance of anode materials in lithium-ion batteries[17–19]. A series of anode materials, including SnO_2-PPy[20], Sn-PPy[18], Si-PPy[17,21], C-PPy[22], and TiO_2-PPy[23,24], have been synthesised and shown enhanced electrical performance in the lithium-ion battery system. Conductive PPy can effectively buffer the volume changes during the cycling process and increase the conductivity of the active materials[25–27]. Meanwhile, the PPy also can connect isolated particles, acting as an efficient host matrix to prevent cracking and pulverization on the surface of electrodes[18,26,28,29]. To the best of our knowledge, however, there have been no reports to date on the synthesis of germanium-conducting polymer composite for application as anode in lithium-ion batteries. In this paper, we have fabricated amorphous nanostructured Ge particles on the surface of PPy through one simple reduction reaction in aqueous solution and investigated the electrochemical properties of the Ge-PPy composite as negative electrode material in the lithium-ion battery.

Results

Physicochemical characterization. X-ray diffraction (XRD) patterns obtained from the pristine nano-Ge and Ge-PPy are shown in Fig. 1(a). The two broad diffraction peaks obtained from the samples are readily indexed to diamond-like cubic Ge (JCPDS card No. 65-0333), which means that the samples present a disordered (amorphous) structure. This result is similar to those reported by Wu et al. for Ge nanoparticle synthesis[30]. The diffraction pattern of the Ge-PPy matches well with the pristine Ge, indicating the presence of Ge and that no impurity was introduced into the composite.

Fig. 1(b) displays the Raman spectra of the bare Ge, PPy and Ge-PPy composite, using laser excitation at 632.8 nm. The Raman peak of the Ge around 293 cm^{-1} in both the pristine material and the composite is asymmetric and has an extended tail at low frequencies, which means that the diameters of the Ge particles should be less than 28 nm[31]. The peaks of the bare PPy located between 800 cm^{-1} and 1700 cm^{-1} are in good agreement with the typical Raman modes of PPy[32]. In this range, the 988 cm^{-1} benzoid band indicates that certain sites of the PPy chain are in the reduced state, whereas the vibrational mode at 931 cm^{-1}, assigned to a C-H out-of-plane deformation of the quinoid form, is related to the oxidize sites[33]. For the intermediate phase in the as-prepared bare PPy, where different vibrational modes assigned to the reduced and the oxidised forms coexist, the polaron is the dominant species. After coating with Ge nanoparticles, the 932 cm^{-1} band remains sharp, while the intensity of the benzoid band at 986 cm^{-1} increases slightly. Simultaneously, the Raman spectrum of the Ge-PPy composite displays the low intensity of the benzoic bands of vC = C at 1531 cm^{-1}, and a significant sharp quinoid form band of vC = C is observed at 1602 cm^{-1}, which is characteristic of the oxidized state of PPy[33,34]. Even after stirring in $NaBH_4$ solution for 3 h, these spectral features indicate that most PPy chains are still at intermediary oxidation levels. Compared with the PPy in reduced state, oxidized PPy is considered as a more effective additive for the lithium-ion battery, due to its electrical repulsion between positive charges present on neighbouring sites, which allows the opening of channels and the penetration of counter-ions[35].

For quantifying the amount of Ge in the composite, thermogravimetic analysis (TGA) was carried out in air. The samples were heated from 50°C to 700°C at a rate of 10°C min^{-1}. Fig. 1(c) presents the TGA curve of the Ge-PPy composite along with that of pure PPy. As can be seen, the PPy content was totally burned out during the heating process, while the Ge in the composite was oxidized into GeO_2 with increasing temperature. The equation is presented below:

$$Ge + O_2(\text{heated to } 700^{\circ}C) \rightarrow GeO_2 \quad (1)$$

So the final product is entirely converted to GeO_2, from which the content of Ge can be calculated. Through using this method, it was estimated that the amount of Ge in the Ge-PPy was about 69.0 wt.%.

The morphologies of the samples were characterized by scanning and transmission electron microscopy (SEM and TEM). The SEM

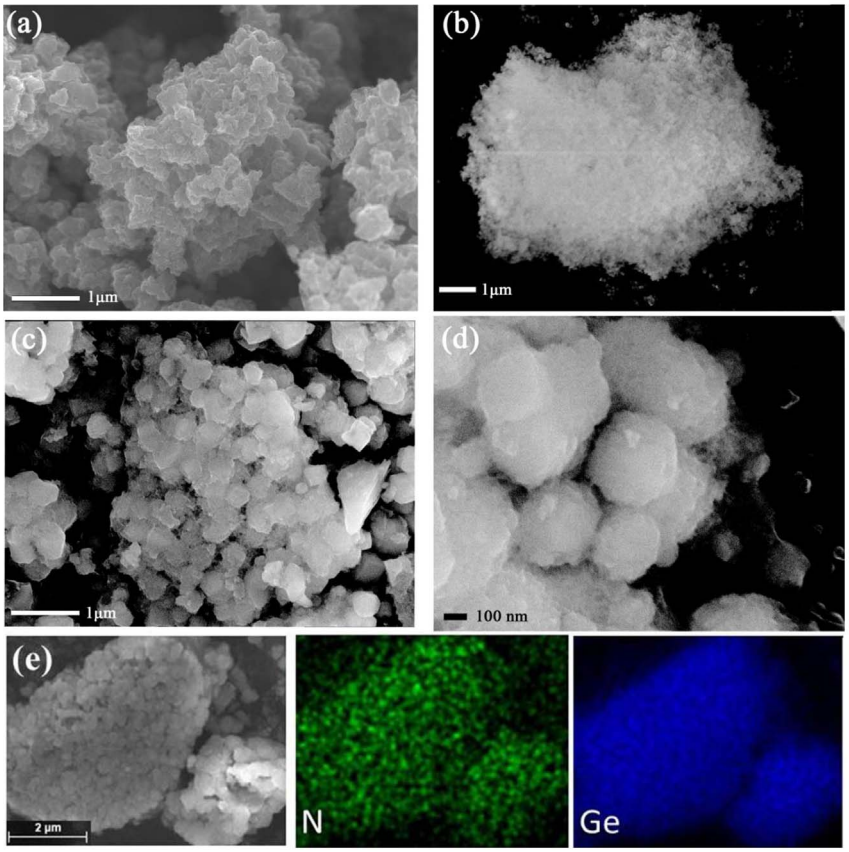

Figure 2 | **SEM images of (a) PPy, (b) Ge nanoparticle, (c, d) Ge-PPy composite, and (e) energy dispersive X-ray mapping of the Ge-PPy composite for the elements Ge and N.**

image of the PPy (Fig. 2a) shows micrometer-sized particles consisting of ~200 nm PPy particles. Fig. 2b reveals that the pristine Ge particle size is extremely small and that these primary particles have clustered into large agglomerates. After coating with Ge nanoparticles, the particles become spherical, and the diameters are increased to about 400 nm (Fig. 2c). With a further increase in magnification, it can be clearly observed that the surfaces of the composite particles (Fig. 2d) have become rough and have some small particles attached. These small particles could be Ge nanoparticles. Another important feature of the composite is that serious agglomeration of Ge nano-

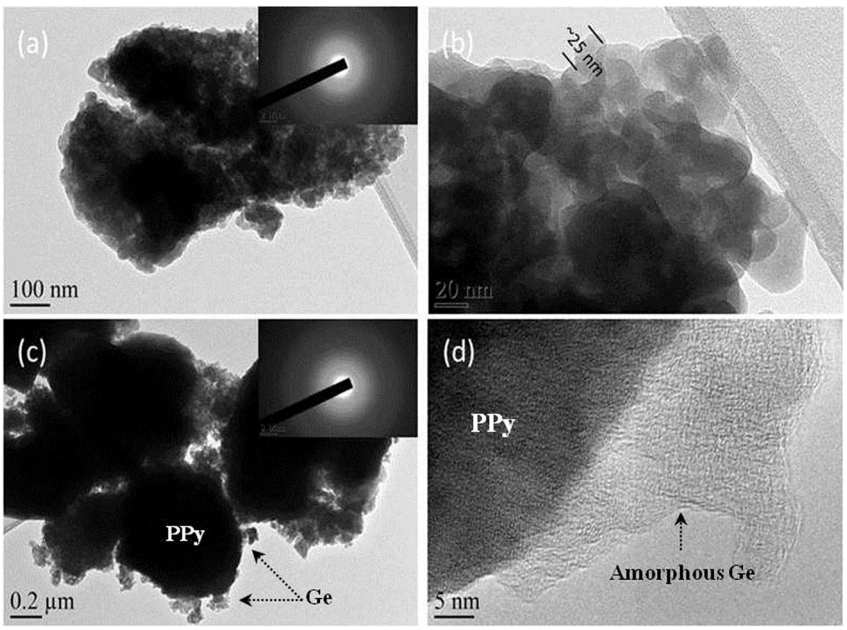

Figure 3 | **TEM images obtained from the pristine Ge (a, b) and the Ge-PPy composite (c, d).** The insets in (a) and (c) are the corresponding SAED patterns.

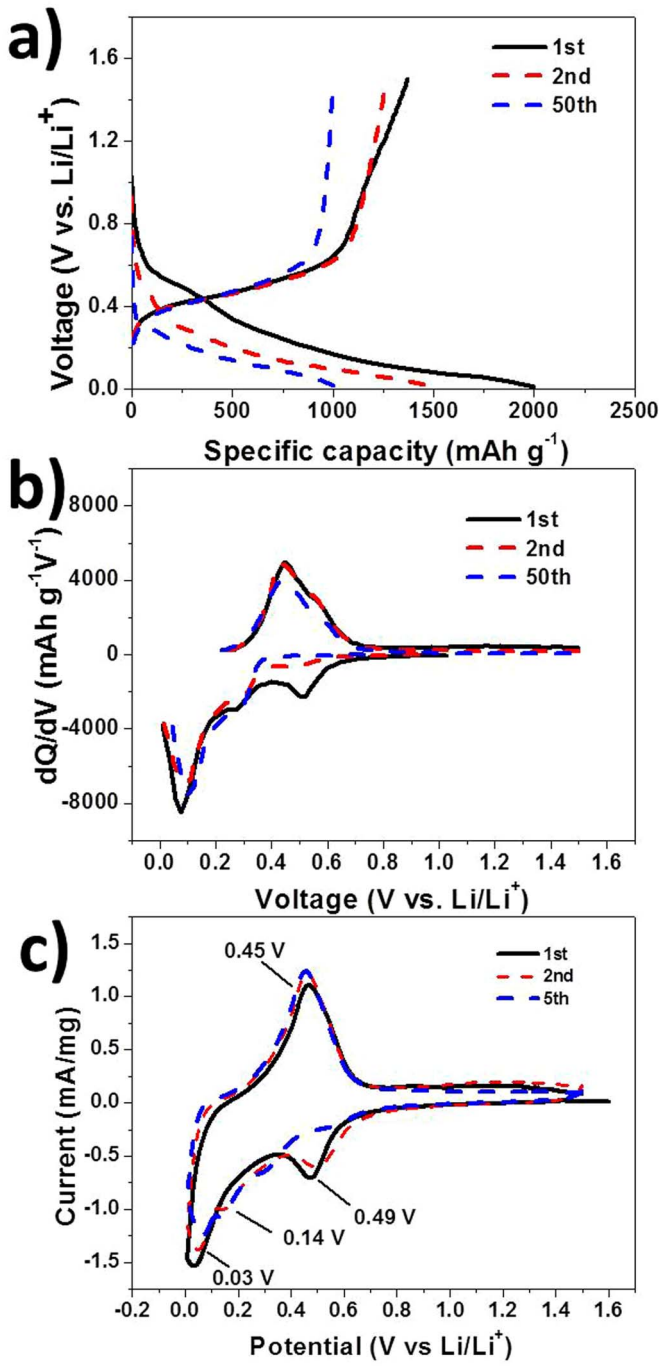

Figure 4 | Charge-discharge curves of Ge-PPy composite for selected cycles (a), dQ/dV plots of Ge-PPy (b), and cyclic voltammograms of Ge-PPy (c); scanning rate: 0.1 mV/S.

particles is relieved, because the PPy can act as a barrier to reduce the gathering of Ge nanoparticles during the Ge-PPy synthesis.

To further investigate the distribution of the Ge in the particles, energy dispersive spectroscopy (EDS) mapping was performed, and the results are shown in Fig. 2(e). The element N is associated with PPy, and the bright regions indicate that the Ge and N are distributed uniformly throughout the sample, which means that the Ge nanoparticles have uniformly coated the surfaces of the PPy.

More highly magnified TEM images of the pristine Ge and Ge-PPy samples are shown in Fig. 3. TEM combined with selected area electron diffraction (SAED: Fig. 3(a) and (c) inset images) confirmed that both the pristine nano-Ge and the Ge in the composite are, in fact, amorphous. Examination of the pristine amorphous Ge at high magnification (Fig. 3b) indicates that the individual Ge particles are around 5–20 nm in diameter and have clustered into larger agglomerates, as is consistent with the SEM results. TEM examination also revealed that the PPy particles connect individual nanosized Ge particles in the Ge-PPy composite (Fig. 3c). A high resolution image of the edges of the PPy particles (Fig. 3d) demonstrates that the amorphous Ge nanoparticles completely cover the individual PPy regions.

Electrochemical properties. Galvanostatic discharge-charge testing between 0–1.5 V at 0.2 C was carried out to investigate the electrical reactivity of the samples. For the PPy electrode, the cell fails during the first discharge period (Fig. S1 in the Supporting Information), which demonstrates that PPy possesses no capacity and no electrochemical activity towards Li in this potential range. Therefore, we calculated the specific capacity based on the weight of Ge in the Ge/PPy composite separately to understand the performance of the Ge particles. The 1st, 2nd, and 50th cycle charge-discharge curves of the Ge-PPy that were collected are shown in Fig. 4(a). The voltage profile and differential capacity data corresponding to the charge and discharge curves are also presented in Fig. 4(b). Several cathodic peaks can be observed in the cycling, which represent the stepwise lithium alloying reaction to form Li_xGe alloys. After 50 cycles, the cathodic peaks at 0.18 V and 0.32 V remain sharp and similar to those in the 2nd cycle, suggesting stability in the reversibility and kinetic activities for Li^+ insertion/extraction of the electrode made from Ge-PPy. To identify all the electrochemical reactions, the electrochemical response was also measured for the Ge-PPy composite by cyclic voltammetry at 0.1 mV s^{-1}. The typical cyclic voltammograms of the Ge-PPy nanocomposite for the 1st, 2nd and 5th cycles, which are shown in Fig. 4(c), are in accordance with previous reports for Ge electrode[7,36]. The broad peaks at around 0.49 V and 0.32 V in the second cathodic curve can be attributed to the conversion from Ge to Li_9Ge_4. The small peak at 0.14 V is likely to be related to the formation of Li_7Ge_2. As the potential approaches 0 V, a big peak starts to appear, indicating the formation of $Li_{15}Ge_4$ and $Li_{22}Ge_5$. The whole discharge (lithiation) reaction can be expressed as a three-step process based on the following reactions:

$$Ge \rightarrow Li_9Ge_4 \rightarrow Li_7Ge_2 \rightarrow Li_{15}Ge_4 + Li_{22}Ge_5 \qquad (2)$$

During Li-ion extraction from Li_xGe, only one single broad peak response around 0.46 V is observed, which agrees with what has been reported in the literature[7,15]. In addition, no additional peaks are detected in the cyclic voltammetery curves of Ge-PPy. This confirms that the PPy is not involved in electrochemical reactions during Li-ion intercalation/deintercalation processes and is only providing paths for electrical conduction[28,29,37].

The battery performances of the samples were tested at various current densities. Initially, the galvanostatic discharge-charge capacity and coulombic efficiency of pristine Ge and Ge-PPy were measured in the voltage range of 0.01–1.50 V with a current density of 320 mA g^{-1} (Fig. 5a). The first discharge capacity of the pure Ge electrode was 1506 mAh g^{-1}, corresponding to an initial coulombic efficiency of 59.3%. This particularly high irreversible discharge capacity mainly comes from the huge formation of solid electrolyte interphase (SEI)[18]. The nano-sized morphology of the particles also plays a significant role, with the utilization of small particles being enhanced by their larger surface area and shorter diffusion length for the lithium intercalation process[10], although the advantages of particle size do not remain stable for long periods of time. As mentioned above, nano-germanium particles would be likely to aggregate severely during the Li^+ insertion, thus leading to poor coulmbic efficiency in the first cycle. Furthermore, as the cycle number increases, the mechanical stresses induced by the volume changes

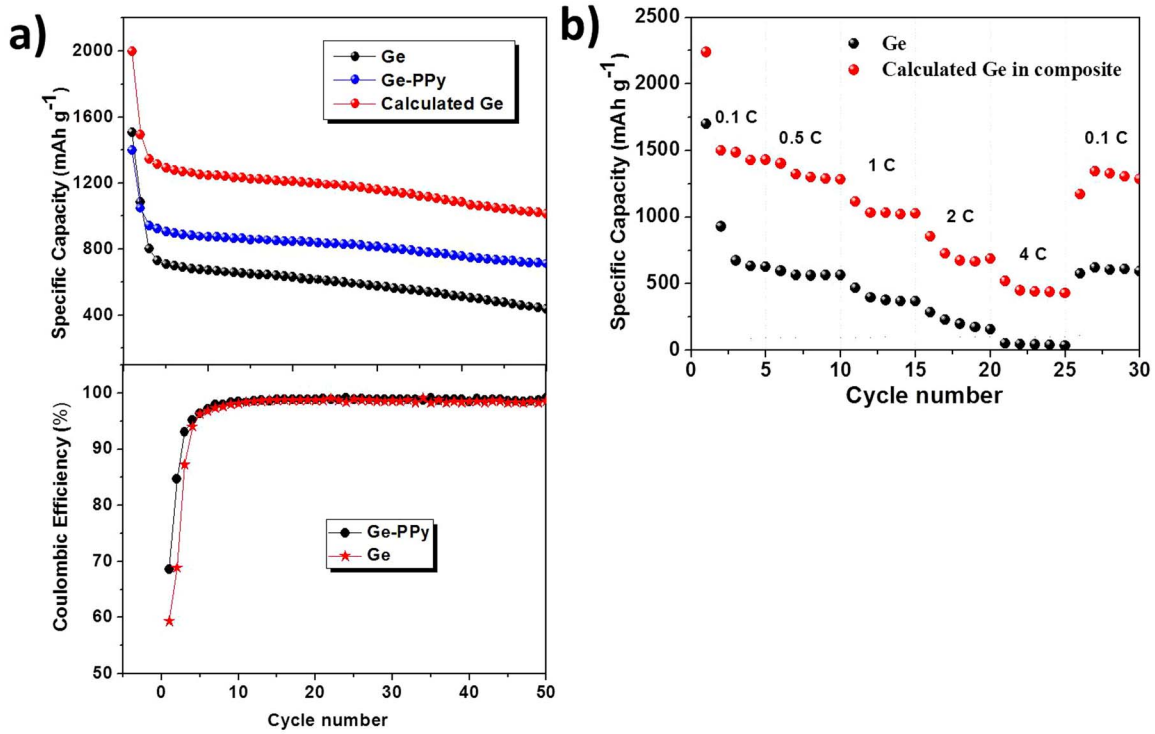

Figure 5 | (a) Discharge capacity and coulombic efficiency of Ge and Ge-PPy composite electrodes at 320 mA g^{-1} (0.2 C). (b) Rate capability of Ge and Ge-PPy composite at various current densities between 0.01 V and 1.50 V vs. Li/Li^+.

would result in pulverization and delamination of the electrode structure, leading to low coulmbic efficiency and poor cycling life[8]. Therefore, the discharge capacity of pristine Ge decreases rapidly and continuously, declining to only 437 mAh g^{-1} over 50 cycles, which is only approximately 29% of the initial capacity. On the other hand, it can be seen that the Ge-PPy composite electrode shows great enhancement of the capacity retention, based on both the composite and the calculated contribution of the pure Ge. The initial capacity of the Ge nanoparticle contribution calculated for the Ge-PPy composite electrode reaches up to 2024 mAh g^{-1}, with a relatively high coulombic efficiency of 68.6%, and after 5 cycles, the coulombic efficiency retains a steady value between 89 and 99%. The difference in the initial coulombic efficiency is mainly due to the PPy, which suppress solid electrolyte interphase (SEI) formation in the first cycle[7,36]. Simultaneously, the Ge nanoparticles are electrical connected with the porous PPy so that more Ge nanoparticles will contribute to the capacity and the electronic transport can be enhanced. Thus, the discharge capacity of Ge in Ge-PPy composite is sustained at around 1029 mAh g^{-1} after 50 cycles at 0.2 C, corresponding to capacity retention of 50.8%. These results demonstrate that the added PPy allows a greater utilization in capacity of the Ge nanoparticles and enhances the cycling performance. Compared to some carbon-supported Ge materials in previous reports, with capacities of around 600 mAh g^{-1} under similar testing conditions[15,38], it can be speculated that the PPy plays a more important role in that enhanced electrochemical activity, although its capacity contribution is negligible in negative electrode for the lithium-ion battery.

A comparison of the performances at higher power rates for both samples (with and without PPy) is also presented in Fig. 5(b). The electrode capacities were measured after 5 cycles at various current densities of 0.1 C, 0.5 C, 1 C, 2 C, and 4 C (1C = 1600 mA g^{-1}) in an ascending order, and back to 0.2 C in 35 cycles. The discharge capacities calculated for the Ge nanoparticles in the composite were measured to be 1420 mAh g^{-1} at 0.5 C, 1300 mAh g^{-1} at 1 C, 865 mAh g^{-1} at 2 C, and 406 mAh g^{-1} at 4 C. When the cycling rate was returned back to 0.1 C after 30 cycles at different rates, the composite electrode still could deliver 1360 mAh g^{-1}. In contrast, strikingly poor high-rate capability is observed for the pristine Ge electrode. It should be pointed out that the rate capability of Ge-PPy is still not as good as for some Ge-based materials recently reported, such as Ge-carbon nanocomposite with 600 mAh g^{-1} at 40 C[5], or Ge thin film electrode with 800 mAh g^{-1} at 1000 C[7]. Nevertheless, the enhanced high-rate performance is comparable to the most research on Ge electrodes combined with graphene[15], mesocarbon microbeads[38], or other carbonaceous materials[39].

In order to further verify that the PPy is responsible for the good conductivity of the cells with the Ge-PPy electrodes, electrochemical impedance measurements were conducted on working electrodes in the fully discharged state. The Nyquist plots obtained for the pure Ge and Ge-PPy before and after 50 cycles were compared and are presented in Fig. 6 (A). It is found that the cells present one small semicircle before cycling, and the impedance is 23 Ω and 49 Ω for Ge-PPy composite and pristine Ge, respectively. In addition, two compressed semicircles are shown in the enlarged high-frequency impedance curves after cycling (Fig. 6(B)), indicating increased impedances. The high-frequency intercept of the high frequency semicircle reflects the uncompensated resistance, R_e, which is the solution resistance between the working and reference electrode. The film resistance associated with the higher frequency semicircle, R_{film}, is assigned to lithium-ion diffusion through surface films. The semicircle in the middle frequency range indicates the charge-transfer resistance (R_{ct}), relating to charge transfer through the electrode/electrolyte interface. The values for the electrodes after cycling calculated from the diameters of the semicircles in the Nyquist plots are summarized in Table S1 (Supporting information). The uncompensated resistance (R_e) of Ge-PPy is smaller than that of the Ge electrode due to the decreased resistance between the active material and the electrolyte from the introduction of PPy. From comparison the diameters of the semicircles, the values of R_{film} and R_{ct} of the composite electrode are both lower than those for the pristine Ge electrode, indicating that the conducting PPy can significantly increase electrical conductivity for the Ge nanoparticles. This

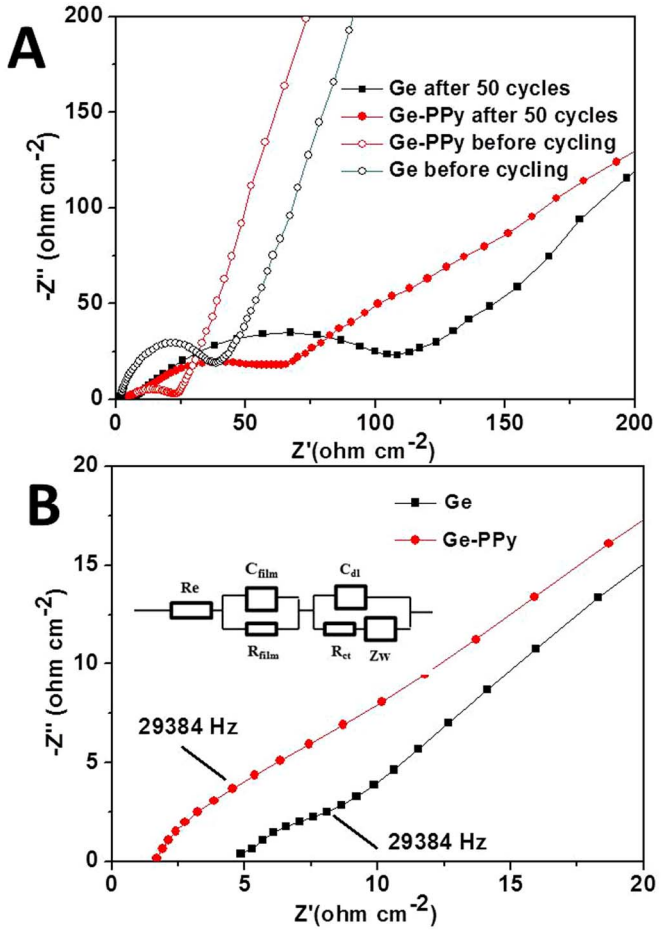

Figure 6 | (A) Nyquist impedance plots of the Ge and Ge-PPy composite electrodes before and after 50 cycles. (B) Enlargement of (A) in the high frequency range of the electrodes after 50 cycles. The inset in (B) is the equivalent circuit used.

is because the conjugation of the single and double bonds alternating within the oxidized PPy macromolecular architecture allow the extra electrons in a conjugated system free to be roamed or move through the polymer chain, which could induce electrical conductivity. Through *p*-doping, the electrical conductivity of PPy can even reach the level of a few tenths of 1 S/cm[40,41], even though it is only around 1 $\times$ 10^{-2} S/cm for crystalline germanium. Accordingly, the introduction of PPy can decrease the charge transfer resistance for the electrode.

To confirm that the Ge-PPy electrode still retained robust mechanical and electrical support after cycling, SEM images of the electrodes fabricated from the Ge and Ge-PPy composite were collected before and after cycling to directly analyse any changes in the microstructure or morphology of the particles during cycling. The surfaces of both electrodes before cycling are similar (Fig. 7(a, b)). After 50 cycles, however, there are large agglomerations of particles 10 μm in size and clearly visible cracks in the bare Ge electrode (Fig. 7c). From Fig. 7d, it can be observed that PPy can protect the electrode from pulverization, but there are still some clearly visible cracks on the surface of the electrode. It can be deduced that PPy not only act as a conductive host matrix, but also work as a binder to prevent the pulverization and delamination of the active material on the surface of the electrode during lithium alloying and de-alloying. We need to point out that PPy core still cannot protect the Ge nanoparticles from cracking. This is because the Ge nanoparticles are only attached on the surface of the PPy, so the PPy core cannot relieve the huge volume change by Ge agglomeration.

Discussion

A novel nanostructured Ge-PPy composite has been successfully fabricated by a simple chemical reduction method and demonstrated to be a promising anode material for lithium-ion batteries. After amorphous Ge nanoparticles were coated on the PPy surface, improved cycling performance and high rate capacity were achieved. The enhanced electrochemical performance can be attributed to the conductive PPy core, which not only can provide efficient electronic pathways for Ge nanoparticles, but also buffers the pulverization and delamination of the electrode caused by the huge volume changes of Ge nanoparticles during lithium alloying and de-alloying. We also expect our strategy to also be useful for fabricating metal nanopar-

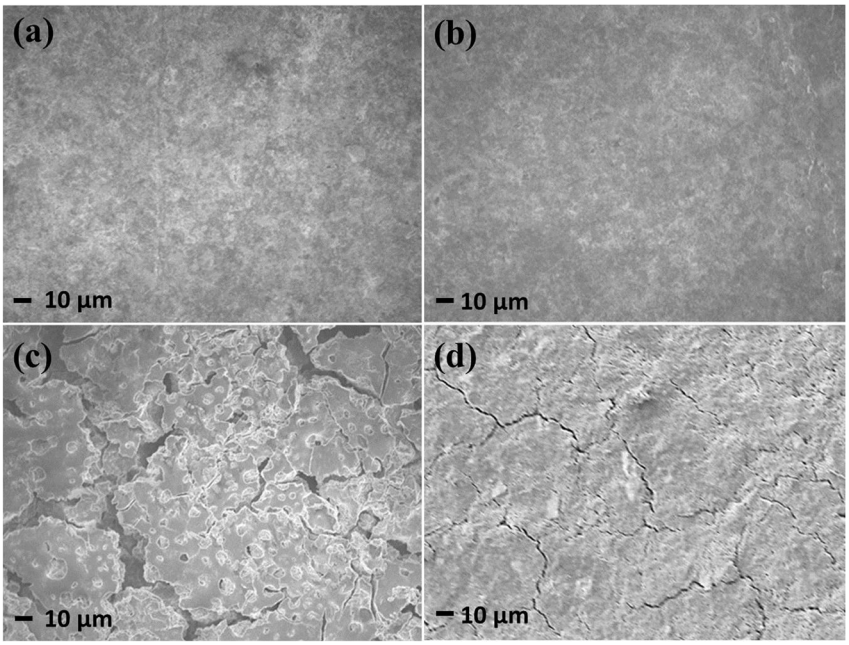

Figure 7 | SEM images of the surfaces of Ge (a, c) and Ge-PPy (b, d) electrodes before (a, b) and after 50 cycles (c, d).

ticles on conducting polymer surface structures, which will be of general interest and have influence in other fields.

Methods

PPy powders were synthesised by chemical oxidation in an aqueous solution. 1 g pyrrole monomer and 0.96 g sodium p-toluenesulfonate (PTS Na) were dispersed in distilled water. Then an oxidizing agent iron chloride ($FeCl_3$) aqueous solution was added drop wise to initiate the polymerization. The PPy was achieved after stirring for 12 h, as indicated when the suspension became black. The products were obtained by filtering and washing with deionized water, and then drying them under vacuum at 60°C for 12 h.

The Ge nanoparticles were prepared by a one-step aqueous reaction. 0.26 g GeO_2 and 0.01 g polyvinylpyrrolidone (PVP) were dissolved completely in 10 mL 0.15 M NaOH solution, and then the pH of the solution was adjusted to 7 with 0.5 M HCl. Then, aqueous $NaBH_4$ solution was added under strong magnetic stirring in a water bath at 60°C. After 3 h, a dark brown suspension was formed, and then the resultant powders were obtained by centrifugation, washed with deionized water several times and dried in a vacuum for 12 h. For the preparation of Ge-PPy composite, the as-prepared PPy powders (50 mg) were dispersed in the solution before reaction.

X-ray diffraction (XRD) analysis was carried out using a GBC MMA generator and diffractometer with Cu Kα radiation and a graphite monochromator. Raman spectroscopy was conducted to characterize the as-prepared PPy and the PPy in the composite, using a JOBIN YVON HR800 Confocal Raman system with 632.8 nm diode laser excitation on 300 lines mm^{-1} grating at room temperature. Thermogravimetric analysis (TGA) was performed using a SETARAM analyzer (France) in air from 50°C to 700°C to determine the amount of PPy in the sample. The morphology and electrochemical properties of the samples were investigated using a JEOL 7500 field emission scanning electron microscope (SEM) with a JEOL energy dispersive spectroscopy (EDS) system. Transmission electron microscopy (TEM) was conducted on a JEOL2011 analytical instrument. The Raman characteristics of samples were investigated using a JOBIN YVON HR800 confocal Raman system with 632.8 nm laser diode excitation on 300 lines/mm grating at room temperature.

The electrodes were prepared using 80 wt.% active materials, 10 wt.% carbon black, and 10 wt.% sodium carboxymethyl cellulose (CMC) in distilled water to form homogeneous slurry. The slurry was spread onto pieces of copper foil. The coated electrodes were dried in a vacuum oven at 100°C for 24 h, and then compressed at a rate of 300 kPa. The electrodes were assembled into CR 2032 coin-type cells in an Ar-filled glove box, using lithium metal as the counter electrode and 1 M $LiPF_6$ in ethylene carbonate/dimethyl carbonate (EC/DMC, 1/1 by volume) as the electrolyte. The cells were cycled between 1.50 V and 0.01 V at a constant current density of 320 mA g^{-1} (0.2 C) on a Land battery tester at 25°C. Different current rates, ranging from 160 mA g^{-1} (0.1 C) to 6400 mA g^{-1} (4.0 C), were also used to measure the electrochemical response. Electrochemical impedance spectroscopy (EIS) and cyclic voltammetry were carried out using a Biologic VMP3 electrochemical workstation.

1. Armand, M. & Tarascon, J. M. Building better batteries. *Nature* **451**, 652–657, doi:10.1038/451652a (2008).
2. Whittingham, M. S. Lithium Batteries and Cathode Materials. *Chem. Rev.* **104**, 4271–4302, doi:10.1021/cr020731c (2004).
3. Lee, H. & Cho, J. Sn78Ge22@Carbon Core−Shell Nanowires as Fast and High-Capacity Lithium Storage Media. *Nano Lett.* **7**, 2638–2641, doi:10.1021/nl071022n (2007).
4. Cui, L. F., Ruffo, R., Chan, C. K., Peng, H. L. & Cui, Y. Crystalline-Amorphous Core-Shell Silicon Nanowires for High Capacity and High Current Battery Electrodes. *Nano Lett.* **9**, 491–495, doi:10.1021/nl8036323 (2009).
5. Seng, K. H., Park, M.-H., Guo, Z. P., Liu, H. K. & Cho, J. Self-Assembled Germanium/Carbon Nanostructures as High-Power Anode Material for the Lithium-Ion Battery. *Angew. Chem.* **124**, 5755–5759, doi:10.1002/ange.201201488 (2012).
6. Wang, Y., Wu, M., Jiao, Z. & Lee, J. Y. Sn@CNT and Sn@C@CNT nanostructures for superior reversible lithium ion storage. *Chem. Mater.* **21**, 3210–3215, doi:10.1021/cm900702d (2009).
7. Graetz, J., Ahn, C. C., Yazami, R. & Fultz, B. Nanocrystalline and thin film germanium electrodes with high lithium capacity and high rate capabilities. *J. Electrochem. Soc.* **151**, A698–A702, doi:10.1149/1.1697412 (2004).
8. Chan, C. K., Zhang, X. F. & Cui, Y. High capacity Li ion battery anodes using Ge nanowires. *Nano Lett.* **8**, 307–309, doi:10.1021/nl0727157 (2008).
9. Winter, M. & Besenhard, J. O. Electrochemical lithiation of tin and tin-based intermetallics and composites. *Electrochim. Acta* **45**, 31–50, doi:http://dx.doi.org/10.1016/S0013-4686(99)00191-7 (1999).
10. Magasinski, A. *et al.* High-performance lithium-ion anodes using a hierarchical bottom-up approach. *Nat. Mater.* **9**, 353–358, doi:10.1038/nmat2725 (2010).
11. Yang, L. C., Gao, Q. S., Li, L., Tang, Y. & Wu, Y. P. Mesoporous germanium as anode material of high capacity and good cycling prepared by a mechanochemical reaction. *Electrochem. Commun.* **12**, 418–421 (2010).
12. Jo, G., Choi, I., Ahn, H. & Park, M. J. Binder-free Ge nanoparticles-carbon hybrids for anode materials of advanced lithium batteries with high capacity and rate capability. *Chem. Commun.* **48**, 3987–3989 (2012).
13. DiLeo, R. A. *et al.* Hybrid Germanium Nanoparticle-Single-Wall Carbon Nanotube Free-Standing Anodes for Lithium Ion Batteries. *J. Phys. Chem. C.* **115**, 22609–22614, doi:10.1021/jp205992w (2011).
14. DiLeo, R. A., Ganter, M. J., Raffaelle, R. P. & Landi, B. J. Germanium-single-wall carbon nanotube anodes for lithium ion batteries. *J. Mater. Res.* **25**, 1441–1446, doi:10.1557/jmr.2010.0184 (2010).
15. Chockla, A. M. *et al.* Electrochemical Lithiation of Graphene-Supported Silicon and Germanium for Rechargeable Batteries. *J. Phys. Chem. C.* **116**, 11917–11923, doi:10.1021/jp302344b (2012).
16. Cheng, J. S. & Du, J. Facile synthesis of germanium-graphene nanocomposites and their application as anode materials for lithium ion batteries. *Crystengcomm* **14**, 397–400, doi:10.1039/c1ce06251d (2012).
17. Chew, S. Y. *et al.* Novel nano-silicon/polypyrrole composites for lithium storage. *Electrochem. Commun.* **9**, 941–946, doi:10.1016/j.elecom.2006.11.028 (2007).
18. Chou, S. L. *et al.* Tin/polypyrrole composite anode using sodium carboxymethyl cellulose binder for lithium-ion batteries. *Dalton T.* **40**, 12801–12807, doi:10.1039/c1dt10396b (2011).
19. Guo, Z. P., Wang, J. Z., Liu, H. K. & Dou, S. X. Study of silicon/polypyrrole composite as anode materials for Li-ion batteries. *J. Power Sources* **146**, 448–451, doi:10.1016/j.jpowsour.2005.03.112 (2005).
20. Yuan, L. *et al.* Synthesis and characterization of SnO2–polypyrrole composite for lithium-ion battery. *J. Power Sources* **174**, 1183–1187, doi:10.1016/j.jpowsour.2007.06.179 (2007).
21. Du, Z. J. *et al.* Facile fabrication of reticular polypyrrole-silicon core-shell nanofibers for high performance lithium storage. *J. Mater. Chem.* **22**, 11636–11641, doi:10.1039/c2jm31419c (2012).
22. Liang, X. *et al.* A composite of sulfur and polypyrrole-multi walled carbon combinatorial nanotube as cathode for Li/S battery. *J. Power Sources* **206**, 409–413, doi:10.1016/j.jpowsour.2012.01.123 (2012).
23. Lai, C., Li, G. R., Dou, Y. Y. & Gao, X. P. Mesoporous polyaniline or polypyrrole/anatase TiO2 nanocomposite as anode materials for lithium-ion batteries. *Electrochim. Acta* **55**, 4567–4572, doi:10.1016/j.electacta.2010.03.010 (2010).
24. Dziewonski, P. M. & Grzeszczuk, M. Towards TiO2-conducting polymer hybrid materials for lithium ion batteries. *Electrochim. Acta* **55**, 3336–3347, doi:10.1016/j.electacta.2010.01.043 (2010).
25. Park, K. S., Schougaard, S. B. & Goodenough, J. B. Conducting-polymer/iron-redox-couple composite cathodes for lithium secondary batteries. *Adv. Mater.* **19**, 848–850, doi:10.1002/adma.200600369 (2007).
26. Boyano, I. *et al.* Preparation of C-LiFePO4/polypyrrole lithium rechargeable cathode by consecutive potential steps electrodeposition. *J. Power Sources* **195**, 5351–5359, doi:10.1016/j.jpowsour.2010.03.029 (2010).
27. Wang, G. X. *et al.* An investigation of polypyrrole-LiFePO4 composite cathode materials for lithium-ion batteries. *Electrochim. Acta* **50**, 4649–4654, doi:10.1016/j.electacta.2005.02.026 (2005).
28. Feng, C. Q., Chew, S. Y., Guo, Z. P., Wang, J. Z. & Liu, H. K. An investigation of polypyrrole–LiV3O8 composite cathode materials for lithium-ion batteries. *J. Power Sources* **174**, 1095–1099, doi:10.1016/j.jpowsour.2007.06.190 (2007).
29. Chew, S. Y. *et al.* Low-Temperature Synthesis of Polypyrrole-Coated LiV[sub 3]O[sub 8] Composite with Enhanced Electrochemical Properties. *J. Electrochem. Soc.* **154**, A633–A637 (2007).
30. Wu, J. H. *et al.* One-step aqueous solution synthesis of Ge nanocrystals from GeO2 powders. *Crystengcomm* **13**, 3674–3677, doi:10.1039/c1ce05191a (2011).
31. Zhang, Y. F. *et al.* Germanium nanowires sheathed with an oxide layer. *Phys. Rev. B* **61**, 4518–4521 (2000).
32. Furukawa, Y., Tazawa, S., Fujii, Y. & Harada, I. Raman spectra of polypyrrole and its 2,5-13C-substituted and C-deuterated analogues in doped and undoped states. *Synthetic Met.* **24**, 329–341, doi:http://dx.doi.org/10.1016/0379-6779(88)90309-8 (1988).
33. Santos, M. J. L., Brolo, A. G. & Girotto, E. M. Study of polaron and bipolaron states in polypyrrole by in situ Raman spectroelectrochemistry. *Electrochim. Acta* **52**, 6141–6145, doi:http://dx.doi.org/10.1016/j.electacta.2007.03.070 (2007).
34. Genoud, F., Guglielmi, M., Nechtschein, M., Genies, E. & Salmon, M. ESR study of electrochemical doping in the conducting polymer polypyrrole. *Phys. Rev. Lett.* **55**, 118–121 (1985).
35. Otero, T. F., Grande, H. & Rodríguez, J. A new model for electrochemical oxidation of polypyrrole under conformational relaxation control. *J. Electroanal. Chem.* **394**, 211–216, doi:http://dx.doi.org/10.1016/0022-0728(95)04033-K (1995).
36. Baggetto, L. & Notten, P. H. L. Lithium-Ion (De)Insertion Reaction of Germanium Thin-Film Electrodes: An Electrochemical and In Situ XRD Study. *J. Electrochem. Soc.* **156**, A169–A175, doi:10.1149/1.3055984 (2009).
37. Idris, N. H., Rahman, M. M., Wang, J.-Z., Chen, Z.-X. & Liu, H.-K. Synthesis and electrochemical performance of LiV3O8/carbon nanosheet composite as cathode material for lithium-ion batteries. *Compos. Sci. Technol.* **71**, 343–349, doi:10.1016/j.compscitech.2010.11.025 (2011).
38. Yoon, S., Park, C. M. & Sohn, H. J. Electrochemical characterizations of germanium and carbon-coated germanium composite anode for lithium-ion batteries. *Electrochem. Solid. ST.* **11**, A42–A45, doi:10.1149/1.2836481 (2008).
39. Lee, H. & Cho, J. Sn78Ge22@carbon core-shell nanowires as fast and high-capacity lithium storage media. *Nano Lett.* **7**, 2638–2641, doi:10.1021/nl071022n (2007).

40. Kudoh, Y. Properties of polypyrrole prepared by chemical polymerization using aqueous solution containing Fe2(SO4)3 and anionic surfactant. *Synthetic Met.* **79**, 17–22, doi:http://dx.doi.org/10.1016/0379-6779(96)80124-X (1996).
41. Cohen, Y. S., Levi, M. D. & Aurbach, D. Micromorphological Dynamics of Polypyrrole Films in Propylene Carbonate Solutions Studied by in Situ AFM and EQCM. *Langmuir* **19**, 9804–9811, doi:10.1021/la0350094 (2003).

Acknowledgments

The authors acknowledge the financial support provided by Australian Research Council (ARC) Discovery Project (DP 110103909) and International Cooperation project of Science and Technology Bureau of Guangdong, China (Grant No. 2012B050300004). The authors also thank Dr. Tania Silver for critical reading of the manuscript.

Author contributions

X.G., J.W., Z.S., H.L. and G.C. wrote the main manuscript. D.W. wrote and executed the TEM part. S.C. and K.O. tested the electrochemical performance of the samples as anode materials in Li-ion batteries. C.Z. did the SEM for the samples. W.L. did the Raman testing for the samples. All authors have reviewed the manuscript.

Additional information

Supplementary information accompanies this paper at http://www.nature.com/scientificreports

Competing financial interests: The authors declare no competing financial interests.

How to cite this article: Gao, X. *et al.* Novel Germanium/Polypyrrole Composite for High Power Lithium-ion Batteries. *Sci. Rep.* **4**, 6095; DOI:10.1038/srep06095 (2014).